Encoding and decoding phase information in high-n circular wave packets

S. Yoshida,[1] C. O. Reinhold,[2,3] J. Burgdörfer,[1,3] B. Wyker,[4] and F. B. Dunning[4]
[1]*Institute for Theoretical Physics, Vienna University of Technology, A-1040 Vienna, Austria, EU*
[2]*Physics Division, Oak Ridge National Laboratory, Oak Ridge, Tennessee 37831-6372, USA*
[3]*Department of Physics, University of Tennessee, Knoxville Tennessee 37996, USA*
[4]*Department of Physics and Astronomy and the Rice Quantum Institute, Rice University, Houston, Texas 77005-1892, USA*
(Received 13 January 2010; published 30 June 2010)

We demonstrate theoretically and experimentally the extraction of detailed information on the density matrix of very-high-n (>300) near-circular Rydberg wave packets through Fourier analysis of the quantum beat and quantum revival signals. The remarkably long coherence times associated with circular wave packets facilitate the preservation and read-out of phase information encoded in this matrix. We illustrate the power of the method by determining the angular localization of the components of a wave packet.

DOI: 10.1103/PhysRevA.81.063428 PACS number(s): 32.80.Rm, 32.80.Qk, 32.60.+i

I. INTRODUCTION

A wave packet comprising a superposition of stationary states is characterized by its complex expansion coefficients a_j, i.e., their moduli and phases [1]. For high-lying Rydberg states the density of states is such that the number of parameters required to uniquely characterize a wave packet becomes large. In consequence, controlling the initial preparation of the wave packet as well as later characterizing the evolved state becomes a challenge. Moreover, protecting quantum coherence, i.e., the relative phases between excitation amplitudes, in high-lying states against decoherence is very difficult due to their extreme sensitivity to environmental interactions. However, developing methods for controlled preparation, evolution, and read out of high-n wave packets is attractive for a number of applications, including protocols for coherent control and quantum information storage. In this article, we show that detailed information on the quantum state amplitudes in a superposition of near-circular states involving more than 100 stationary eigenstates $|n,l,m\rangle$ can be retrieved. This is accomplished by constructing carefully tailored wave packets for which the relative phases between adjacent n levels are only weakly dependent on l and m. The present protocol gives access to a subset of off-diagonal density matrix elements that contain information on the relative phases between quantum state amplitudes. Near-circular states are remarkably robust against decoherence, allowing this information to be retained for extended periods. As will be shown, the relative phases of near-circular states correspond to the geometric angle and provide information on the angular localization of the wave packet. By extracting both the phases and population (moduli) of the individual component n levels, a (partial) reconstruction of the wave packet is possible.

The relative phases and populations of quantum-state expansions can be obtained through Fourier analysis of signals obtained using time-dependent pump-probe methods. Such approaches have been used to resolve the vibrational states of molecules [2] or to probe the expansion coefficients of Rydberg wave packets with $n \sim 30$ [3,4]. For higher-n ($n \sim 300$) states protecting the encoded information against decoherence becomes a major challenge due to their sensitivity to external perturbations. Nonetheless, we have recently shown that near-circular wave packets [5] with $l \simeq n$ are surprisingly robust against decoherence with coherence times $\gtrsim 1\mu$s [6], equal to hundreds of Kepler orbital periods. Here we show another remarkable feature of near-circular wave packets: the phases of reduced density matrix elements $\rho_{n,n+1}$ remain well defined, i.e., survive, when traced over l and m states of the wave packet involving nearly a hundred l and m states in each n level. We show that the phases and moduli of the density matrix elements can be extracted from Fourier analysis of the quantum beat signal. In particular, features specific to $n \simeq l \simeq m$ states allow extraction of the dynamical phase angles of the quantum superposition which, we show, coincide with the azimuthal localization angles ϕ_0.

II. FOURIER ANALYSIS OF WAVE PACKET DYNAMICS

The circular wave packets are prepared (see Refs. [5,6] for more details) by first creating quasi-one-dimensional (Q1D) very-high-n potassium Rydberg states oriented along the x axis by direct photoexcitation of selected red-shifted Stark states from the ground state in the presence of a weak ($\sim$400 μV cm^{-1}) dc field [7]. The weak dc field is then turned off and a transverse electric pump field, $F_{\rm pump}$, suddenly applied along the $-y$ axis creating a wave packet that undergoes Stark precession in the xy plane. After a time $T_{\rm pump} = \pi/(3nF_{\rm pump})$ this precession [8] transforms the wave packet to a superposition of high-angular-momentum states ($l \sim m \sim n$)

$$|\Psi(t)\rangle = \sum_n{}' \sum_{l,m}{}' |a_{n,l,m}| e^{-i\Phi_{n,l,m}(t)} |\psi_{n,l,m}\rangle\,, \qquad (1)$$

where $|a_{n,l,m}|$ is the modulus and $\Phi_{n,l,m}$ is the phase of the expansion coefficients (atomic units are used throughout). The primed summation indicates that the sum over n, l, and m is restricted to a narrow range of n (governed by the strength of $F_{\rm pump}$) and $l \sim m \sim n$. Switch-off of the pump field at this time (taken as $t = 0$ for the subsequent field-free evolution) prevents further Stark precession, creating a near-circular wave packet, whose radial wave function peaks near $r \sim n^2 (\sim 5\,\mu$m) and which is localized near the xy plane [spherical harmonics $Y_l^m(\theta,\phi)$ with $l \sim m$ have large amplitudes near $\theta = \pi/2$]. The wave packet is initially fairly uniformly distributed in azimuth, i.e., in ϕ. Localization in azimuth requires the coherent

superposition of several m states with properly aligned phases $\Phi_{n,l,m}$. If, for example, $\Phi_{n,l,m} \simeq m\phi_0$, the wave packet is localized at ϕ_0 with a width determined by the range of m included in the superposition [9]. After switching off the pump field (at $t = 0$), $\Phi_{n,l,m}(t)$ evolves as $\Phi_{n,l,m}(0) - t/(2n^2)$.

The rotating wave packet can be monitored by observing the expectation value of its y (and/or x) coordinates,

$$\begin{aligned}\langle y(t)\rangle &= \sum_{n,l,m}{}' \sum_{n',l',m'}{}' |a_{n,l,m}a_{n',l',m'}| e^{-i(\Phi_{n,l,m}(t)-\Phi_{n',l',m'}(t))} \\ &\quad \times \langle\psi_{n',l',m'}|y|\psi_{n,l,m}\rangle \\ &\simeq \sum_{n,l,m}{}' 2D_{n,l,m}\sin[\Delta\Phi_{n,l,m}(t)] \equiv \sum_{n,l,m}{}' \langle y(t)\rangle_{n,l,m}\,, \quad (2)\end{aligned}$$

where $D_{n,l,m} = |\langle\psi_{n,l,m}|\rho y|\psi_{n,l,m}\rangle|$ is the modulus of the dipole expectation value for a density matrix with element $\langle\psi_{n',l',m'}|\rho|\psi_{n,l,m}\rangle = a_{n,l,m}a^*_{n',l',m'}$ and $\Delta\Phi_{n,l,m}(t) = \Phi_{n+1,l+1,m+1}(t) - \Phi_{n,l,m}(t)$. Here, $D_{n,l,m}$ can be approximated as

$$D_{n,l,m} \simeq |a_{n,l,m}a_{n+1,l+1,m+1}\langle\psi_{n+1,l+1,m+1}|y|\psi_{n,l,m}\rangle|\,, \quad (3)$$

because, for circular states, the dipole matrix elements effectively couple only states satisfying the condition $n' = n \pm 1$, $l' = l \pm 1$, $m' = m \pm 1$. Each component $\langle y(t)\rangle_{n,l,m}$ oscillates harmonically with amplitude $2D_{n,l,m}$ and a time-dependent phase

$$\Delta\Phi_{n,l,m}(t) = \Delta\Phi_{n,l,m}(0) + \Omega_n t\,, \quad (4)$$

where $\Omega_n = 1/(2n^2) - 1/[2(n+1)^2]$ closely matches its classical counterpart ($\Omega_n \simeq n^{-3} = \omega_n$) for large n. The entire wave packet thus behaves as an ensemble of "classical" electrons in different n, l, m states. The localization condition $\Phi_{n,l,m} = m\phi_0$ is equivalent to the condition $\Delta\Phi_{n,l,m} = \phi_0$ and corresponds to the situation where all the components in Eq. (2) within a single n shell remain in phase at all times. If this condition is satisfied, $\langle y(t)\rangle$ displays strong harmonic oscillations that can be probed experimentally. However, each n-component evolves with a different angular frequency leading to dephasing. Unlike true classical ensembles, the wave packet is governed by a discrete energy spectrum leading to quantum revivals when a finite number of n levels are "dephased" from each other by $2j\pi$ at $t = 2j\pi/(\Omega_n - \Omega_{n+1}) \simeq 2j\pi n^4/3$ ($j = 1,2,3,\ldots$).

Given the relatively simple form of Eq. (2), information on both the phase and modulus can be extracted from a Fourier transform of $\langle y(t)\rangle$

$$c_n = \frac{1}{T}\int_0^T \langle y(t)\rangle e^{i\Omega_n t}dt \simeq \sum_{l,m}{}' D_{n,l,m}e^{-i\Delta\Phi_{n,l,m}(0)+i\pi/2}\,, \quad (5)$$

provided that T is sufficiently long to resolve individual n levels, i.e., $T \gg 2\pi/(\Omega_n - \Omega_{n+1})$. When (as here) the components exhibit angular localization, i.e., the $\Delta\Phi_{n,l,m}(0)$ are nearly independent of l and m, the complex expansion coefficients can be factorized as

$$c_n \simeq e^{-i\Delta\Phi_{n,l,m}(0)+i\pi/2}\sum_{l,m}{}' D_{n,l,m}\,. \quad (6)$$

Since the dipole matrix elements for circular states are nearly independent of l and m, $|\langle\psi_{n+1,l+1,m+1}|y|\psi_{n,l,m}\rangle| \simeq n^2/2$, and the sum of off-diagonal elements of the density matrix can be determined as

$$\left|\sum_{l,m}{}'\langle\psi_{n+1,l+1,m+1}|\rho|\psi_{n,l,m}\rangle\right| = \frac{2}{n^2}\sum_{l,m}{}' D_{n,l,m}\,. \quad (7)$$

This quantity approximates, for a fully coherent ensemble, the geometric mean of the occupation probabilities for the n and $n+1$ levels. Alternately, it can be interpreted as the probability for a "classical" electron to evolve with angular frequency $\omega_n = n^{-3}$. [Note that use of Fourier analysis to extract azimuthal angles $\phi_0 = \Delta\Phi_{n,l,m}$ and values of $|c_n|$ works only for n components localized in ϕ. Those n components not localized in ϕ produce no time dependence in the observable $\langle y(t)\rangle$.]

III. COMPARISON WITH EXPERIMENT

The evolution of $\langle y(t)\rangle$ can be probed experimentally through ionization using a pulsed field directed along the y axis. Because the survival probability mirrors the expectation value of the electron y coordinate at the application of the pump pulse [10], measurements of the survival probability versus the time delay, $\tau_{\rm delay}$, after turn off of $F_{\rm pump}$ provide information on the time development of $\langle y(t)\rangle$. In practice, an ionization pulse with amplitude 100 mV cm^{-1}, duration 6 ns, and rise and fall times of ~0.3 ns (sufficient to ionize ~50% of the initial Rydberg atoms) is employed and $\tau_{\rm delay}$ is varied in steps of 0.4 ns. Results obtained using an incoherent mix of red-shifted Stark states ($n_i \sim 305$) and a pump field $F_{\rm pump} = -5$ mV cm^{-1} applied for $T_{\rm pump} = 85$ ns are presented in Fig. 1. The initial buildup of strong periodic oscillations in survival probability demonstrates the creation of a wave packet strongly localized in azimuth in near-circular Bohr-like orbit about the nucleus [5,11]. While this localization is subsequently lost through dephasing strong quantum revivals are evident at later times.

The localization seen in Fig. 1 indicates that the pump pulse yields relative phases $\Delta\Phi_{n,l,m}(0)$ that, while depending on n, are relatively independent of l and m. This strong correlation (coherence) in phase can be understood using a simple classical picture [12]. Sudden application of $F_{\rm pump}$ (directed along the $-y$ axis) leads to an energy transfer $\Delta E = y_i F_{\rm pump}$, where

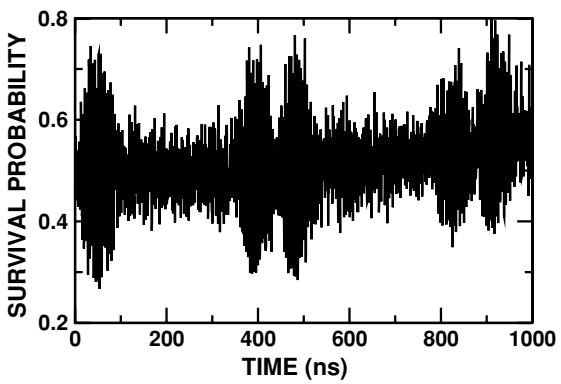

FIG. 1. Measured survival probabilities as a function of the time delay between turn off of the pump field and application of a 6-ns, 100-mV cm^{-1} probe pulse in the $-y$ direction for a mix of parent Q1D $n_i = 303$ and 305 atoms (see text). A pump field $F_{\rm pump} = -5$ mV cm^{-1} of 85-ns duration is employed.

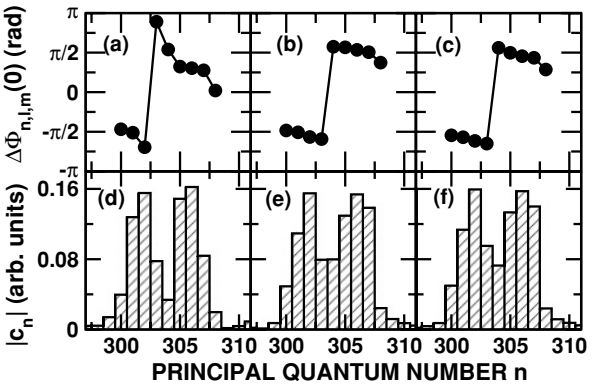

FIG. 2. Amplitude and phase of the Fourier transform [Eq. (5)] of [(a and d)] the measured survival probability (Fig. 1), [(b and e)] the simulated survival probability (see Ref. [6]), and [(c and f)] the simulated $\langle y(t)\rangle$. The histograms [(d–f)] indicate the amplitude of the (normalized) Fourier expansion coefficients $|c_n|$ and the symbols [(a–c)] the relative phase $\Delta\Phi_{n,l,m}(0) \sim i\log(c_n/|c_n|) + \pi/2$. The simulations use an incoherent mix of Q1D red-shifted Stark states in the $n = 303$ and $n = 305$ manifolds (see text). The pump and the probe fields are as in Fig. 1.

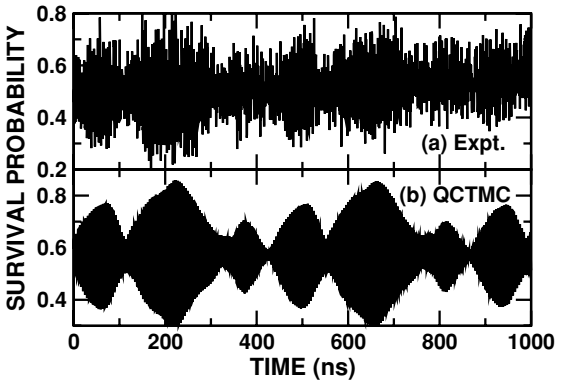

FIG. 3. (a) Measured and (b) calculated survival probabilities as a function of the time delay between turn off of the pump field and application of a 6-ns, 100-mV cm^{-1} probe pulse in the $-y$ direction for a mix of parent Q1D $n_i = 304$ and 306 atoms (see text). A pump field $F_{\text{pump}} = -2$ mV cm^{-1} of 170-ns duration is employed.

y_i is the initial electron coordinate but this is small as the Q1D state is initially aligned with the x axis, i.e., $y_i \sim 0$. However, at the turn off of F_{pump} the electron probability density is fairly uniformly distributed around a near circular orbit of radius $r \sim n_i^2$. Projection of this distribution onto the y axis yields a probability density distribution that is strongly peaked near $y_f \sim \pm n_i^2$ (y_f is the final electron coordinate at $t = 0$). On turn off of F_{pump} that portion with $y_f \sim n_i^2$, i.e., with azimuthal angle $\phi \sim \pi/2$, gains energy $\Delta E = n_i^2|F_{\text{pump}}|$ moving it to a higher n. That portion with $y_f \sim -n_i^2$, i.e., with azimuthal angle $\phi \sim -\pi/2$, loses energy moving it to a lower n level. Thus for each of these "extreme" final states the quantum number n is directly related to the initial angle $\phi_0(n)$ or, equivalently, the relative phase $\Delta\Phi_{n,l,m}$ which is, to a good approximation, independent of l and m. For n values between the extrema, two values of ϕ, $\phi_0(n)$ and $\pi - \phi_0(n)$, are associated with each n. The corresponding component wave packets have two peaks in ϕ and are more "delocalized."

The spatial information encoded in the modulus $|c_n|$ and phase $\Delta\Phi_{n,l,m}(0) \simeq \phi_0(n)$ can be extracted through Fourier analysis of the data (see Fig. 2). $|c_n|$ features two peaks near $n = 306$ and $n = 302$. The corresponding phases $\Delta\Phi_{n,l,m}$ are $\phi_0(n \simeq 306) \simeq \pi/2$ and $\phi_0(n \simeq 302) \simeq -\pi/2$, as expected for a two-component wave packet (or Schrödinger cat state) whose components are initially localized on opposite sides of the nucleus [6]. Figure 2 also includes the results of simulations undertaken using the quantized classical trajectory Monte Carlo (QCTMC) method described elsewhere [6]. These simulations employ as an initial state a mix of restricted microcanonical ensembles mimicking the experimentally realized Q1D state. For $n_i \sim 305$, the splitting of the n_i and $n_i - 2$ Rydberg levels is similar to that of the ground $F = 2$ and $F = 1$ hyperfine levels (~461.7 MHz) allowing simultaneous excitation of Q1D $n = 303$ and 305 states having very similar spatial characteristics. As evident from Fig. 2, Fourier analysis of the calculated survival probabilities provides results that agree with those obtained experimentally. Calculations of $\langle y(t)\rangle$ were also undertaken and Fourier analyzed. The Fourier spectra are similar to those obtained from the calculated survival probabilities (see Fig. 2), confirming that the behavior of the survival probability mimics that of $\langle y(t)\rangle$. The data demonstrate that measurements of survival probabilities can provide both the magnitude of the $\Delta n = 1$ coherences as well as their phase angle, which coincides with the geometric azimuthal angle. This is all the more remarkable given that the overall initial degree of coherence is quite small $(\text{Tr}\rho^2/(\text{Tr}\rho)^2 < 0.01)$.

Figure 3 shows survival probabilities measured using a mix of $n_i = 304$ and 306 states following application of a smaller pump field $F_{\text{pump}} = -2$ mV cm^{-1} for $T_{\text{pump}} \sim 170$ ns. The small size of F_{pump} limits the maximum energy transfer that accompanies its turn-on or turn-off such that it becomes comparable to the splitting of the $n_i = 304$ and 306 levels. The observed buildup of large oscillations in survival probability again points to transient localization and creation of Bohr-like wave packets, and strong periodic revivals are present. As evident from Fig. 4 Fourier analysis of the data yields two

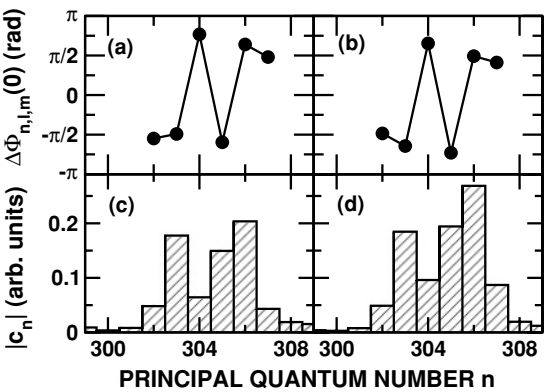

FIG. 4. Amplitude and phase of the Fourier transform of the [(a and c)] measured and [(b and d)] calculated survival probabilities in Fig. 3. The histograms [(c and d)] indicate the amplitude of the (normalized) Fourier expansion coefficients $|c_n|$ and the symbols [(a and b)] the relative phase $\Delta\Phi_{n,l,m}(0)$.

peaks in $|c_n|$ but the width of the overall n distribution is substantially smaller than seen in Fig. 2, consistent with the use of a smaller pump field. However, while in Fig. 2 the phase varies only weakly across each peak and increases by π from one to the other, in Fig. 4 a phase jump of π occurs within each peak. This indicates that each peak derives from just one of the initial parent states. Indeed, the relative weight of the two peaks as determined by the integral over $|c_n|$, $\sim 40\%$ for $n \sim 303$ and $\sim 60\%$ for $n \sim 306$, is consistent with the weights expected for a statistically populated incoherent ensemble of ground hyperfine levels. This interpretation is supported by QCTMC simulations. The calculated beat and revival pattern agrees with the experimental data (see Fig. 3) as do the corresponding Fourier transforms. This agreement is remarkable given the susceptibility of very high n Rydberg states to even modest perturbations.

IV. SUMMARY AND OUTLOOK

Circular wave packets feature a direct correlation [Eq. (2)] between their spatial distribution and the complex expansion coefficients of Eq. (1). Thus, with proper manipulation of the spatial distribution by, for example, careful control of the rise or fall times of the pump field or by breaking up the pump field into segments and varying the intermediate time delays, it should be possible to imprint information into the superposition which can be subsequently retrieved through measurements of its time evolution. As demonstrated, this can be accomplished even with an initial statistical ensemble of states. Fourier spectroscopy is quite robust against statistical errors. Even when the measured survival probabilities have limited statistics and display large fluctuations, the Fourier transform converges relatively quickly because the statistical noise frequencies can be separated from the Kepler orbital frequency by recording (as done here) the survival probability with a much finer time step than the Kepler period. The present findings suggest future opportunities to exploit this excitation protocol for quantum information storage and entanglement of hyperfine and spin degrees of freedom with the spatial localization of a Rydberg wave packet using coherently excited hyperfine states.

ACKNOWLEDGMENTS

This research was supported by the NSF under Grant No. 0650732, the Robert A. Welch foundation under Grant No. C-0734, the OBES, US DOE to ORNL, which is managed by the UTBatelle LLC under Contract No. AC05-00OR22725, and by the FWF (Austria) under SFB016.

[1] J. Ahn, T. C. Weinacht, and P. H. Bucksbaum, Science **287**, 463 (2000).
[2] N. F. Scherer, R. J. Carlson, A. Matro, M. Du, A. J. Ruggiero, V. Romero-Rochin, J. A. Cina, G. R. Fleming, and S. A. Rice, J. Chem. Phys. **95**, 1487 (1991).
[3] R. R. Jones and M. B. Campbell, Phys. Rev. A **61**, 013403 (1999).
[4] J. Ahn, D. N. Hutchinson, C. Rangan, and P. H. Bucksbaum, Phys. Rev. Lett. **86**, 1179 (2001).
[5] J. J. Mestayer, B. Wyker, J. C. Lancaster, F. B. Dunning, C. O. Reinhold, S. Yoshida, and J. Burgdörfer, Phys. Rev. Lett. **100**, 243004 (2008).
[6] C. O. Reinhold, S. Yoshida, J. Burgdorfer, B. Wyker, J. J. Mestayer, and F. B. Dunning, J. Phys. B **42**, 091003 (2009).
[7] C. L. Stokely, J. C. Lancaster, F. B. Dunning, D. G. Arbó, C. O. Reinhold, and J. Burgdörfer, Phys. Rev. A **67**, 013403 (2003).
[8] I. C. Percival and D. Richards, J. Phys. B **12**, 2051 (1979).
[9] E. A. Shapiro, Sov. Phys. JETP **91**, 449 (2000).
[10] B. E. Tannian, C. L. Stokely, F. B. Dunning, C. O. Reinhold, and J. Burgdörfer, Phys. Rev. A **64**, 021404(R) (2001).
[11] F. B. Dunning, J. J. Mestayer, C. O. Reinhold, S. Yoshida, and J. Burgdörfer, J. Phys. B **42**, 022001 (2009).
[12] C. O. Reinhold, S. Yoshida, J. Burgdörfer, J. J. Mestayer, B. Wyker, J. C. Lancaster, and F. B. Dunning, Phys. Rev. A **78**, 063413 (2008).